UNDERSTANDING CATION-π INTERACTIONS THROUGH GAS-PHASE CHARGE-TRANSFER ELECTRONIC SPECTROSCOPY

by

DYLAN S. ORR

(Under the Direction of Michael A. Duncan)

ABSTRACT

Gas-phase charge-transfer electronic spectroscopy was utilized to probe Ag^+(benzene) and Ag^+(toluene) complexes. These ions were generated via laser vaporization in a pulsed supersonic expansion then mass-selected and photodissociated using a tunable UV-Vis OPO laser. Electronic excitation spectra were measured via a metal-to-ligand charge-transfer process in which the organic cation was exclusively generated. Measuring the wavelength dependence of photodissociation resulted in broad, featureless absorptions that were identified as the charge-transfer state and a silver excited electronic state. The threshold for the dissociation energy of both complexes was determined from an excitation to the repulsive wall of the charge-transfer excited states. Computational work was completed in tandem using TD-DFT and predicted both excited state absorptions with relative success. These results in combination with previous work illuminated new energetics for the cation-π interactions in these complexes.

INDEX WORDS: Cation- π Interactions, Charge-Transfer Complexes, Photodissociation, Electronic Spectroscopy, Mass Spectroscopy, Gas-Phase

UNDERSTANDING CATION-Π INTERACTIONS THROUGH GAS-PHASE CHARGE-TRANSFER ELECTRONIC SPECTROSCOPY

by

DYLAN S. ORR

B.S., University of Georgia, 2016

A Thesis Submitted to the Graduate Faculty of The University of Georgia in Partial Fulfillment of the Requirements for the Degree

MASTER OF SCIENCE

ATHENS, GEORGIA

2022

UNDERSTANDING CATION-Π INTERACTIONS THROUGH GAS-PHASE CHARGE-TRANSFER ELECTRONIC SPECTRSCOPY

by

DYLAN S. ORR

Major Professor:	Michael Duncan
Committee:	Gary Douberly Brandon Rotavera

Electronic Version Approved:

Ron Walcott
Vice Provost for Graduate Education and Dean of the Graduate School
The University of Georgia
August 2022

DEDICATION

I dedicate this work to my friends, family, and colleagues that believed in me and cultivated me into the researcher and person I am today. A special thanks to my brother, Gary, who has always loved and supported me and walked with me down paths I was too frightened to travel alone. To my partner, Lacey, who always loves me even when loving me is difficult and has always truly believed in me. To my mom, Suzanne, whose love and support pushed me to succeed. To my friend and lab partner, Jason, who taught me and was there for me more than he will ever realize. To my niece, Charli, who I've just met but has already inspired me to be a better man. I couldn't have done this without any of you.

ACKNOWLEDGEMENTS

I would like to acknowledge Jason Colley for his help on this project. He helped and explained so much that I wouldn’t have been able to make it through this program without him. I will always cherish the seemingly endless frustrations we shared and overcame. He is a friend, colleague, and teacher that anyone would be lucky to have. I would like to thank Mike Duncan for giving me this opportunity to learn and grow as a researcher. His unending curiosity and persistence has always been admirable and inspiring. He pushed me when I needed to be pushed and I grew as both a person and researcher under his direction. I would like to thank Dr. Gary Douberly and Dr. Brandon Rotavera for being exceptional teachers and mentors. Thank you to the University of Georgia Chemistry department and Georgia Advanced Computing Resource Center for giving me the tools I needed to successfully complete this project.

TABLE OF CONTENTS

Page

CHAPTER

LIST OF TABLES

Page

LIST OF FIGURES

CHAPTER 1

INTRODUCTION

Motivation

Understanding the energetics of cation-π complexes is a complicated process that can be approached in a variety of methods. Cation-π complexes and interactions are important in many different biological processes including molecular distinction, protein folding, antigen-antibody recognition, and mediation of enzyme-substrate binding.[1-12] Organometallic chemistry is ripe with metal-aromatic ions that contain cation-π interactions and thus have been previously studied in great detail.[3-6] More recently, carbon-based nanostructures have been identified as "single site" catalysts that interact and bind under similar circumstances as the smaller organometallic cation- π complexes.[13-17] Due to their importance in almost every field of chemistry and far-reaching applications, benzene containing metal complexes have been studied extensively using many different experimental techniques as well as computational studies.[2,18-62] Learning more about the energetics of cation-π interactions will have far reaching applications for many different fields of study in chemistry. Bond energies, dissociation thresholds limit, and excited electronic states can all be identified by probing the cation- π interaction complexes.

Cation-π Complexes

Cation-π interactions are composed of an electron rich π system, typically an organic compound, interacting with a positively charged metallic ion. Cation-π interactions have an electrostatic component that is typically covalent with transition metals and non-covalent with non-transition metals. This molecular interaction is ubiquitous in organometallic chemistry and biological processes.[1-12] Since it is so common, understanding the structures and energetics of these interactions is a growing field of research with many practical applications. Mass spectroscopy has been used to investigate complexes with cation-π interaction to better understand their vibrational and electronic excitations. Probing a cation-π complex with a UV-Vis photodissociation laser results in identification of electronically excited states. Infrared photodissociation (IR-PD) in combination with computational studies can be utilized to study vibrational excitations and better understand the molecular structure of these complexes. [1,2,6,17-62] Collisional-induced dissociation has been previously utilized by Armentrout and Chen to determine dissociation thresholds which in turn can be used to calculate bond energies.[37,63] It is probable that unquenched metastable excited states produced in the ion formation can result imprecise determination of these dissociation thresholds.

UV-Vis photodissociation spectroscopy has been previously employed to probe the electronic excited states of metal cation complexes with small molecules such as N_2 and O_2 but there are very few studies looking at the electronically excited states of cation-π containing organometallic complexes. There have been some previous excited state electronic studies of these complexes including the Duncan group reporting the electronic spectra of $Mg^+(C_2H_2)$ and $Ca^+(C_2H_2)$.[64,65] Yeh et al. has reported electronic spectra for Ag^+(pyridine) and Ag^+(furan) complexes and Kleiber et al. studied multiple $M^+(C_2H_4)$ complexes.[66-71] In conjunction with electronic spectroscopy, the Duncan group developed a photofragment imaging experiment that utilizes mass-selection to determine the bond energies of ions containing cation-π interactions.[72] With the use of gas-phase supersonically cooled ions it is possible to obtain electronic spectra of cold cation-π metal complexes with more a more accurate threshold for dissociation. Since there are few previous studies focusing specifically on cation-π organometallic compounds this leaves a rich pool of novel molecules to study through electronic photodissociation. Studying these molecules will help researchers better understand the energetics of all metallic cation-π complexes.

Charge-Transfer

Photoinduced charge-transfer has become a rapidly expanding area of study due to the role it plays in energy transfer processes in biological and chemical processes. These processes include organic semiconductors used for solar energy capture as well as the fundamental basis of life on Earth, photosynthesis. They have been documented and studied using photochemistry, spectroscopy, and computational work. Charge-transfer complexes contain one charged molecule that either donates or receive an electron after being electronically excited. This refers to the transfer of an electron from one ligand to another, hence the name charge-transfer. Photoinduced charge-transfer has been previously observed for gas-phase ions and has been studied by several different experimental methods. The Bowers group studied dissociative charge transfer processes in the visible spectra of charge-transfer complexes that reside in the atmosphere.[73-75] The Duncan, Yeh, and Kleiber groups have all studied ionic organometallic processes of dissociate charge transfer processes using photodissociation of gas phase ions.[66-71,76-79] The Duncan group has employed velocity map imaging (VMI) in conjunction with photoinduced dissociation mass spectroscopy to determine kinetic energy release and energetics for photo-induced charge transfer complexes.[72,80]

The basis of charge-transfer organometallic ions comes from the ionization energy of the metal ion and that of the organic ligand. Charge-transfer is seen frequently in these molecules because their ionization energies are close enough that an electron can easily be transferred by a photochemical excitation. In general, metal ions have ionization potentials of 6-9 eV while aromatic organic molecules have ionization potentials of 8-10 eV. Photoinduced charge-transfer is readily seen in the visible and near UV wavelength regions in complexes when the ionization energy difference is 1.5-2 eV. While photoinduced charge-transfer is seen as a photochemical process, it can be utilized as a tool to dig deeper into these complexes to determine structure, bond energy, and where the charge lies in the complex. In electronically excited systems, broad absorptions are documented due to an excitation to the repulsive wall of the charge-transfer excited states. These absorptions can be used to determine the threshold of dissociation energy for charge-transfer complexes. Combining this information with previously known atomic and molecular states, it is possible to deduce new information on the energetic cycles of these unique systems.

Previous Research

Previous work on both Ag^+(benzene) and Ag^+(toluene) has given some key insights into the energetics of these charge-transfer complexes. Armentrout and coworkers employed collisional induced dissociation (CID) to determine bond energies for the Ag^+(benzene) complex but not Ag^+(toluene). They determined a dissociation limit of 35.4 ± kcal/mol.[63] The Duncan group were able to determine a more accurate dissociation limit threshold for Ag^+(benzene) and Ag^+(toluene) charge transfer complexes by using a velocity map imaging (VMI) experiment which determines the kinetic energy release for a more accurate threshold. They concluded the threshold of dissociation for Ag^+(benzene) and Ag^+(toluene) were $< 28.9 \pm 3.2$ and $< 35.9 \pm 3.2$ respectively.[80] They also were the first to scan the electronic spectrum of both complexes but lacked sufficient cooling and tunability in the dye laser which resulted in significantly broader absorptions and thus a less accurate threshold determined by the charge-transfer absorption.[76] None of these experiments resulted in accurate spectroscopic findings thus further research was needed to better understand the energetics of these cation- π charge-transfer complexes as well as unearth any new transitions over an increased range of tunable light.

An interesting component of the cation-π interaction is determining whether the bond is covalent or noncovalent. Looking at previously documented dissociation energies of transition metal-benzene complexes it can be seen that all transition metal-benzene are most likely covalent due to their high dissociation energies. **Table 1** below shows a selection of documented transition metals with the weakest bond of Mn+(benzene) in the range of the energy required to dissociate a covalent bond. The Duncan group reported Ag^+(benzene) being 28.9 +/- 3.2 kcal/mol using VMI as stated above, which is lower than any of the CID reported values of transition metal-benzene complexes but still much stronger than a noncovalent bond.

Table 1: Documented dissociation energies of transition metal ion benzene complexes.

M^+(benzene) dissociation energies	
Metal Ion	Dissociation energy (kcal/mol)
Mn^+	31.8[41]
Cr^+	40.6[41]
Fe^+	49.6[41]
Cu^+	52.1[41]
V^+	55.8[41]
Ni^+	58.1[41]
Co^+	61.1[41]
Ti^+	61.8[41]
Au^+	69.9[83]

CHAPTER 2

EXPERIMENTAL METHODS

Gas-Phase Mass Spectroscopy

Photodissociation time-of-flight gas-phase mass spectroscopy was employed to study the electronic excitations of both Ag^+(benzene) and Ag^+(toluene) complexes. The mass spectrometer is a modified Wiley-McLaren time-of-flight mass spectrometer (TOF-MS) that can be seen in **Figure 1**. The cationic complexes were generated using laser vaporization at 355 nm (Spectra Physics INDI Nd:YAG laser) of a silver rod. The rod was situated in the source chamber equipped with a diffusion pump (Agilent VHS-10) to prevent atmosphere from contaminating the experiment. A cutaway source configuration and rotator rod assembly housed the silver rod in order to reliably generate ions over an extended period of time. The ions were cooled with a supersonic expansion of pulsed argon gas using the offset configuration of the cluster source **(Figure 2)**. Benzene and toluene in liquid form were added to the argon backing line and in combination with the laser vaporization, Ag^+(benzene) and Ag^+(toluene) ions were generated, collisionally cooled, and extracted into a molecular beam for analysis in the mass spectrometer.

Once the ions were extracted into a molecular beam, they were sent to the mass spectrometer chamber for mass selection, photodissociation, and analysis. The mass spectrometer chamber was pumped using a diffusion pump (Agilent VHS-6) to maintain a pressure of approximately 10^{-7} torr. The ions were reflected towards the detector using a series of biased plates. Mass selection occurred via pulsed plates right before the ions are decelerated for photofragmentation in the reflectron. Mass-selection is necessary to be certain the desired ions are the only ones making it through to the photofragmentation section for analysis.

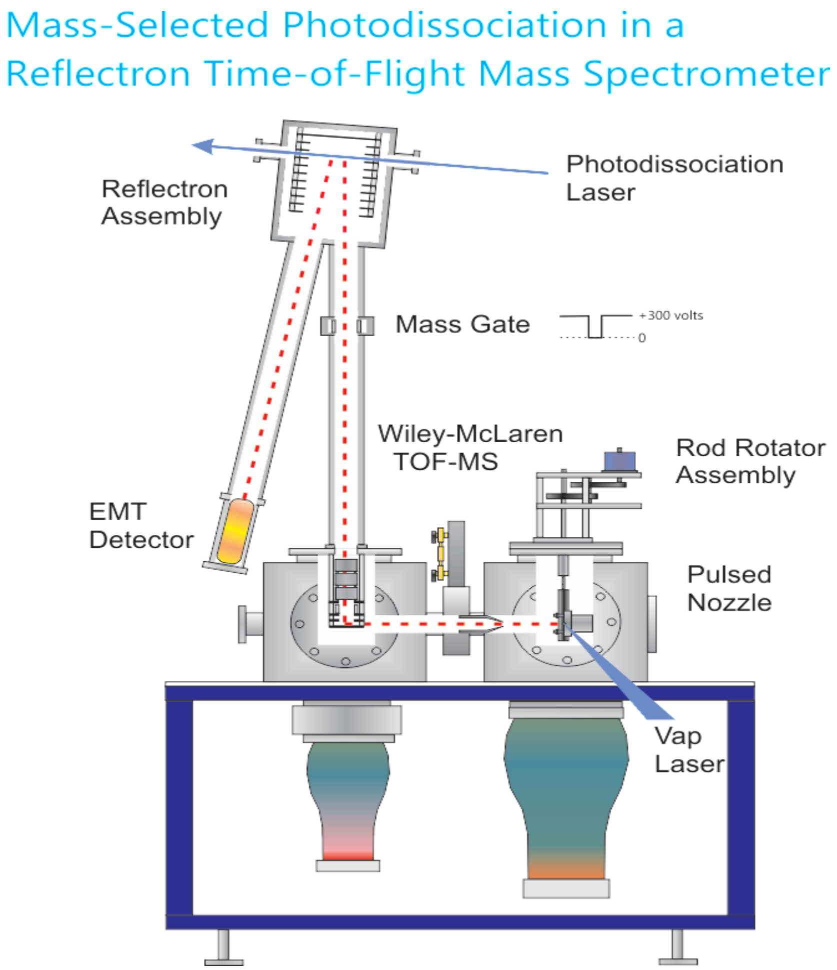
Mass-Selected Photodissociation in a Reflectron Time-of-Flight Mass Spectrometer

Figure 1: Diagram of the molecular beam machine and modified Wiley-McLaren time-of-flight mass spectrometer used for detecting ionic complexes.

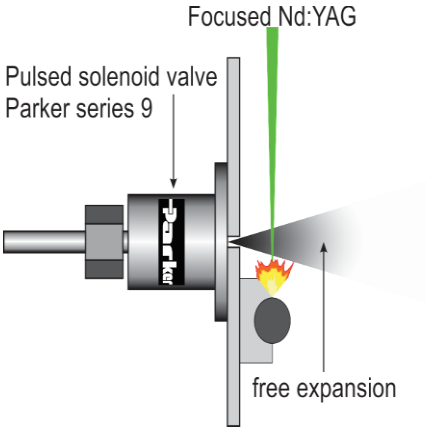

Figure 2: Setup of offset source for ion generation via laser vaporization of a silver rod and supersonically cooled with an argon expansion.

Photodissociation Fragmentation

Photodissociation of the mass-selected ions was achieved using a solid-state tunable UV-visible optical parametric oscillator (UV-vis OPO). The UV-vis OPO (Continuum Horizon II) was pumped using a laser (Continuum Surelite-EX laser). The UV-vis OPO has a tunable range of 192-2750 nm which covered the visible spectrum down to the deep UV. This is a relatively new system that utilizes a combination of OPA crystals in tandem with frequency doubling and mixing to give such a broad range of tunable light without having to use a dye laser. This system can generate linewidths down to approximately 5 cm^{-1}. Wavelengths were calibrated with an Avantes Starline spectrometer.

After mass-selection, Ag^+(benzene) or Ag^+(toluene) ions from the mass chamber were decelerated and photodissociation via the UV-vis OPO. The reflectron is a series of gradually decreasing plates that allow for a parabolic flight path in which the ions could be reliably photodissociated. The reflectron then accelerated the photofragmented ions to an electron multiplier tube (EMT) detector. The “parent” (original ion) and fragment ion intensities were collected using the electron multiplier tube (EMT) detector and an oscilloscope. Comparing the ratio of parent to fragment over a specified wavelength range resulted in generation of the electronic spectra. For both the Ag^+(benzene) and Ag^+(toluene) complexes, the electronic spectra were generated by measuring the loss of benzene and toluene ions. Cationic silver was never seen or measured during the photodissociation of both complexes. The electronic spectra were recorded over the frequency range of 25,000 cm^{-1} to 45,000 cm^{-1} at 0.1 nm, 0.5 nm, and 1 nm linewidths to search for electronic transitions of the cation-π complexes. This was repeated several times to ensure reproducibility and the best 3 scans were averaged for a better noise-to-signal ratio in the final figures. The lower energy side of the charge-transfer excited state was repeatedly scanned and averaged to determine an accurate threshold of dissociation for both complexes.

CHAPTER 3

ELECTRONIC SPECTROSCOPY

Ag^+(benzene)

Ag^+(benzene) ions were produced in the manner discussed in the previous chapter. **Figure 3** shows the mass spectrum of the Ag^+(benzene)$_n$ clustering seen when generating these clusters. The first large peak is the Ag^+ ion with benzene clustering (n=1-3) following.

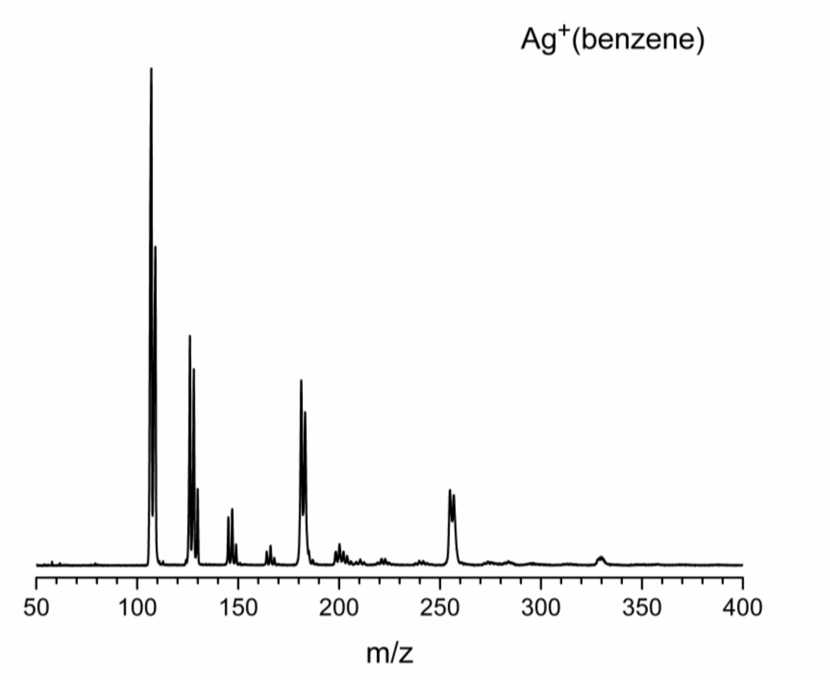

Figure 3: Mass spectrum of Ag^+(benzene)$_{n=1-3}$ clusters.

The Ag^+(benzene) molecules were then mass-selected and fragmented using the UV-vis OPO system described in the proceeding chapter. Silver exists in a near 1:1 isotope mixture of ^{107}Ag and ^{109}Ag so it was expected to see a doublet peak for the initial compound and it was possible to mass-select each isotope as needed. The Ag^+(benzene) complex was mass-selected and photodissociated in the reflectron with tunable light from 200-450 nm. Only the benzene ion was observed in the photodissociation mass spectrum as seen in **Figure 4** below.

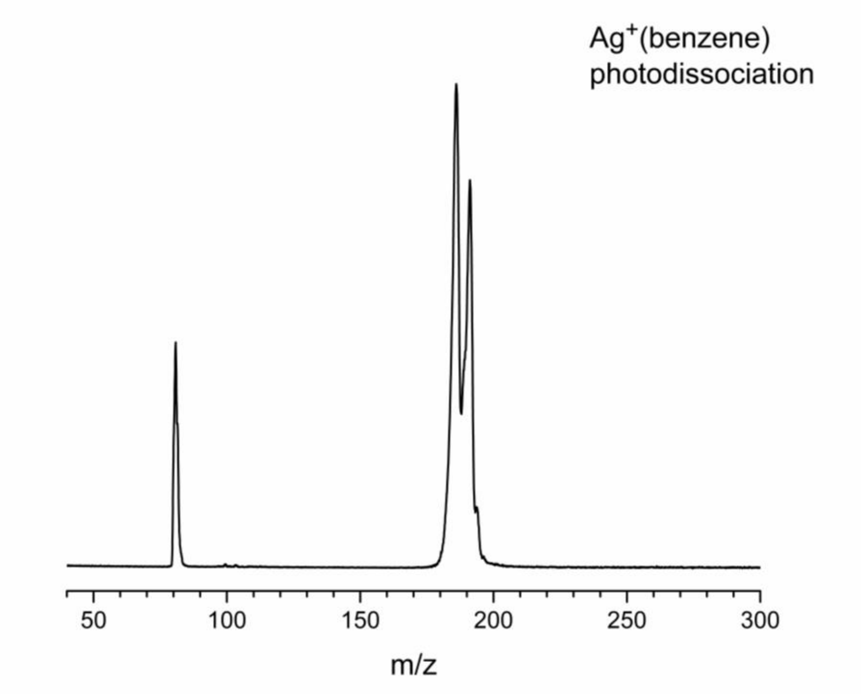

Figure 4: Photofragmentation mass spectrum of Ag^+(benzene) at 355nm.

This was already an unusual result as photodissociation was assumed to generate a combination of both $benzene^+$ and Ag^+ fragment ions. Since only the $benzene^+$ ion was produced, the electronic spectrum was recorded based on the ratio of the intensities of the parent ion (Ag^+(benzene)) to the fragment ion ($benzene^+$). An increase in the fragment ion would be the result of increased photodissociation at that specific wavelength which implies an electronic transition occurs at that energy. Scanning using tunable light from 200-420 nm while measuring the $benzene^+$ fragment loss from Ag^+(benzene) was documented several times and averaged to generate **Figure 5**.

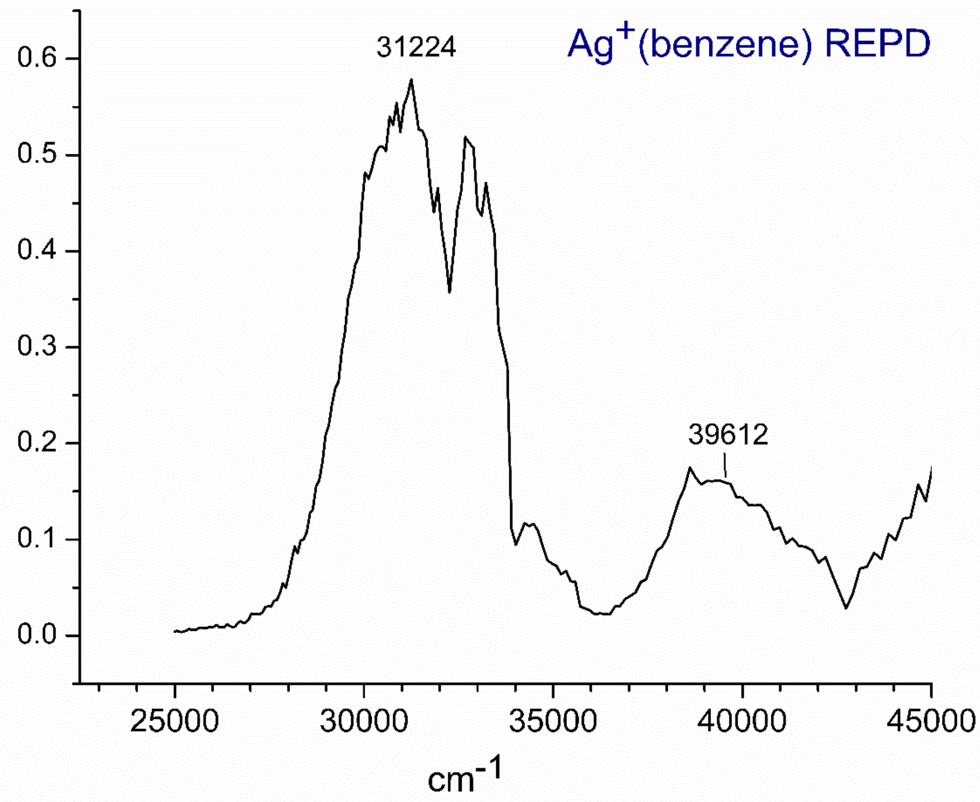

Figure 5: Electronic photodissociation spectrum of the Ag^+(benzene) complex measured by loss of $benzene^+$. The tunable light was scanned over a range of 200-420 nm and at a step size of 0.1nm. The wavelength (nm) was converted to wavenumbers (cm^{-1}).

Two broad absorptions were identified centered at 31,224 cm^{-1} and 39,612 cm^{-1}. It was expected to see a broad absorption for the charge-transfer excited state. The lower energy peak (31,224 cm^{-1}) was assigned to this charge-transfer excited state. The second higher energy peak (39,612 cm^{-1}) was unexpected and was initially theorized to be an excited benzene ligand. Further work including computational studies was needed to correctly assign an electronically excited state to this peak.

Ag^+(toluene)

Ag^+(toluene) ions were produced in the manner discussed in the previous chapter. **Figure 6** shows the mass spectrum of the $Ag^{+(}$toluene)$_n$ clustering seen when generating these clusters. The first large peak is the Ag^+ ion with toluene clustering (n=1-3) following.

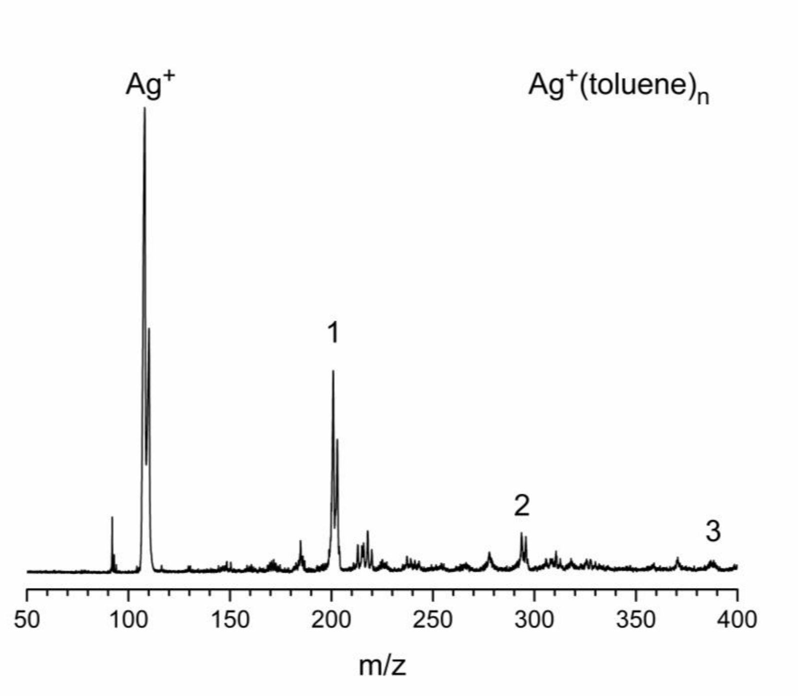

Figure 6: Mass spectrum of Ag^+(toluene)$_{n=1-3}$ clusters.

The Ag^+(toluene) molecules were then mass-selected and fragmented using the UV-vis OPO system as described in the proceeding chapter. The Ag^+(toluene) complex was mass-selected and photodissociated in the reflectron with tunable light from 200-400 nm. Only the toluene ion was observed in the photodissociation mass spectrum as seen in **Figure 7** below.

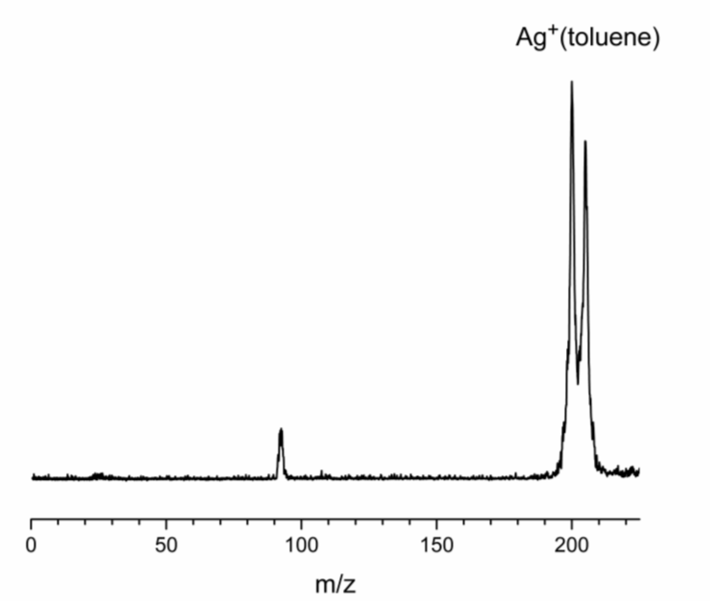

Figure 7: Photofragmentation mass spectrum of Ag$^+$(toluene) at 355 nm.

In agreement with the Ag$^+$(benzene) work, only the toluene$^+$ ion was observed during photodissociation. The electronic spectrum was generated by recording the intensity of the fragment peak (toluene$^+$) compared to the parent peak (Ag$^+$(toluene)). Scanning usable tunable light from 200-400 nm several times was documented as averaged to obtain **Figure 8**.

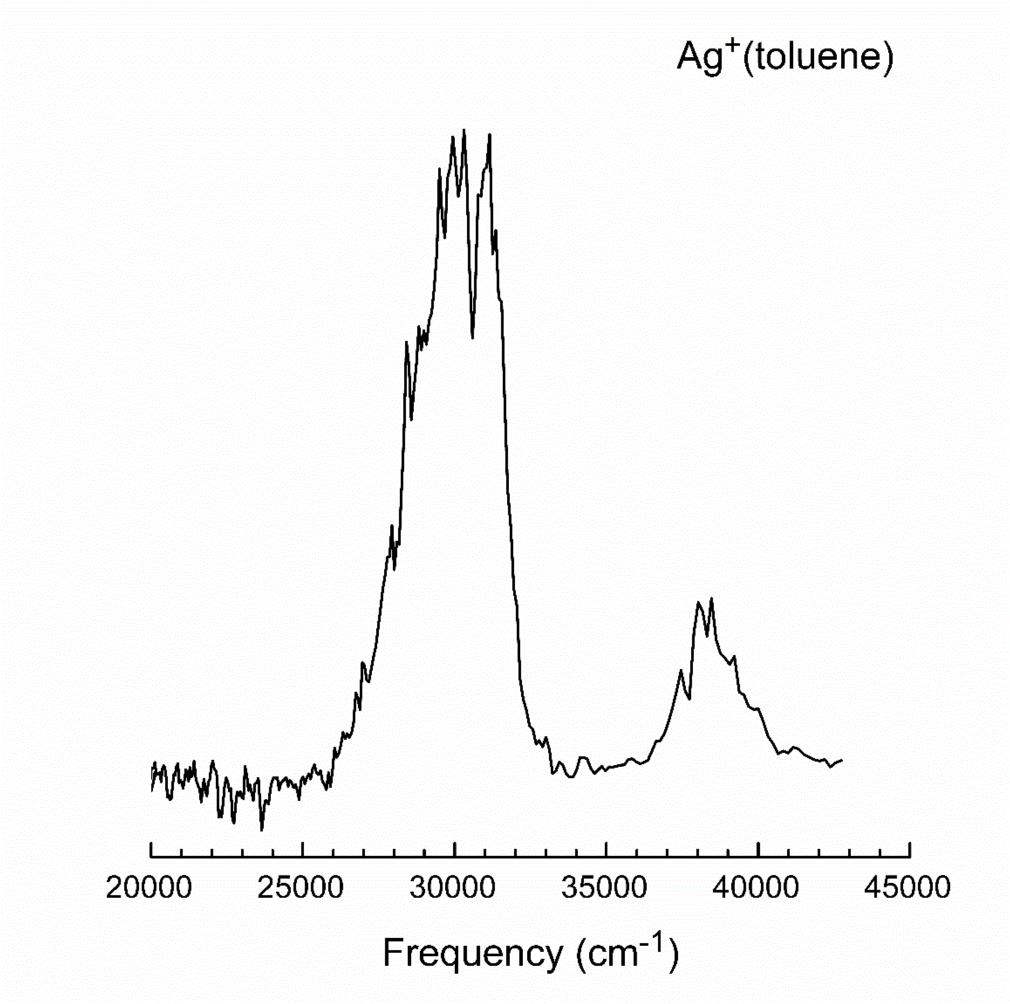

Figure 8: Electronic photodissociation spectrum of the Ag^+(toluene) complex measured by loss of toluene$^+$. The tunable light was scanned over a range of 200-400 nm and at a step size of 0.1nm. The wavelength (nm) was converted to wavenumbers (cm^{-1}).

Similar to Ag^+(benzene), two broad absorptions were identified centered at 29,885 cm^{-1} and 38,417 cm^{-1}. A broad absorption for the charge-transfer excited state was expected. The lower energy absorption (29,885 cm^{-1}) was assigned to this charge-transfer excited state. The second higher energy absorption (38,418 cm^{-1}) was yet again unexpected as it was theorized that the higher energy absorption in Ag^+(benzene) was a charged benzene ligand. Since both cation-π complexes had this peak at relatively the same frequency, the explanation changed from a charged benzene ligand to the common component in both complexes, Ag^+. It was still possible that these higher energy absorptions could be charged ligands since only the hydrocarbon fragment ions were detected. Either way, some strange chemistry occurred during photodissociation that needed to be further studied using computational calculations and a close examination of known excited electronic and molecular states. **Figure 9** below compares the electronic photodissociation spectra of Ag^+(benzene) and Ag^+(toluene).

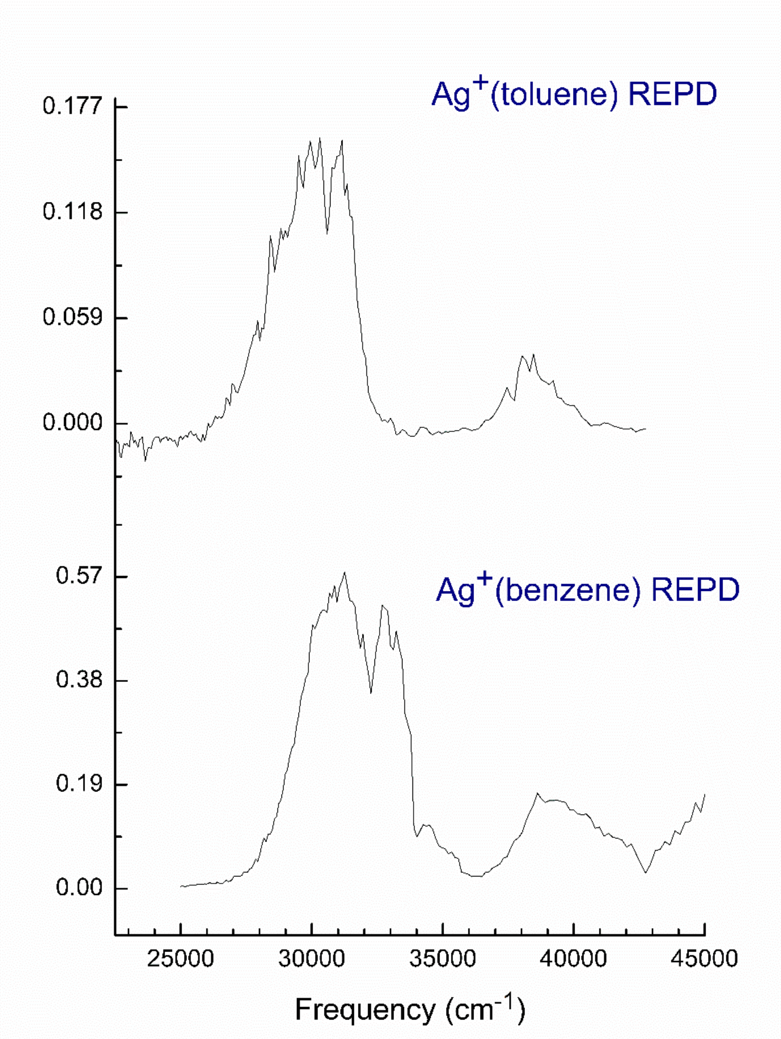

Figure 9: Electronic photodissociation spectra of the Ag^+(toluene) and Ag^+(benzene) complexes. Both complexes have a higher and lower energy absorptions in the same region.

Threshold Determination

Once the charge-transfer excited state absorptions were documented and assigned for the Ag^+(benzene) and Ag^+(toluene) complexes, the lower energy absorption could be further examined to determine the threshold of the dissociation energy of the complexes. The lower energy absorption peaks for both complexes were scanned extensively with a step-size of 0.1nm and averaged to obtain a definitive energy. The Ag^+(benzene) complex had a broad background excitation so it was not possible to determine the threshold by only looking at where there was complete loss of fragment ion. The background excitation had to be corrected for based on the intensity of the fragment ion compared to the parent ion in conjunction with a power correction since the UV-vis OPO system output power changed depending on the wavelength. **Figure 10** shows the lower energy absorption for the Ag^+(benzene) that was used to determine the dissociation limit of 26,368 cm^{-1} or 75.4 kcal/mol.

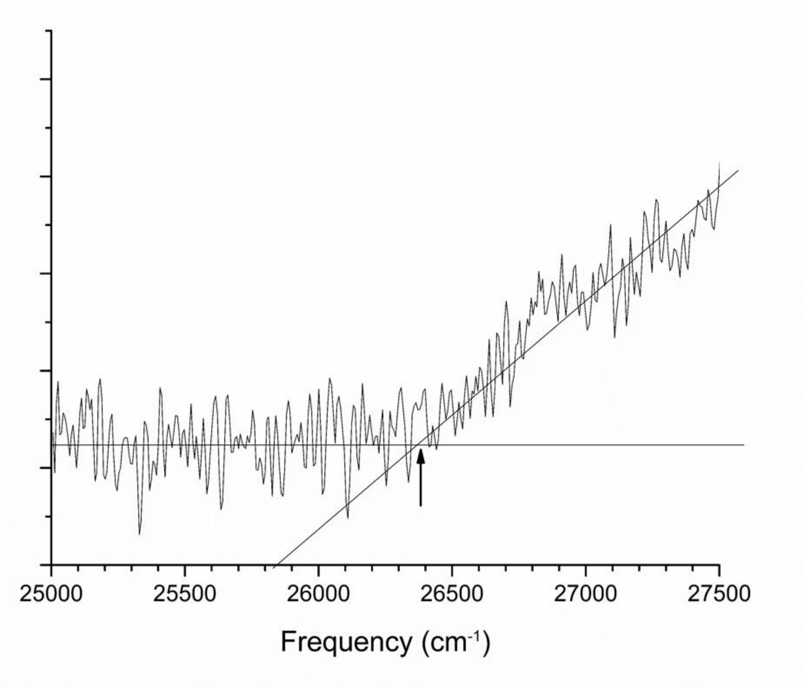

Figure 10: Dissociation threshold of Ag^+(benzene) determined by charge-transfer electronic photodissociation spectroscopy.

The same process just described was used to determine the threshold of dissociation for the Ag^+(toluene) complex. **Figure 11** shows the lower energy absorption for the Ag^+(toluene) that was used to determine the dissociation limit of 25,813 cm^{-1} or 73.8 kcal/mol. Unlike the benzene complex, the toluene complex had a much better signal to noise ratio due to very stable parent signal which allowed for a more precise determination.

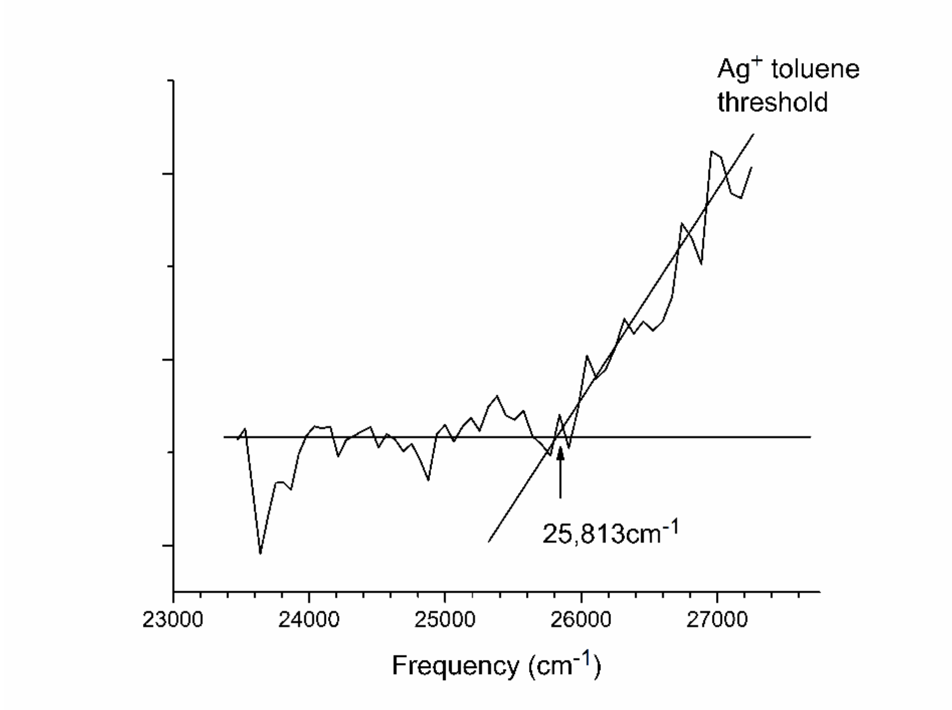

Figure 11: Dissociation threshold of Ag$^+$(toluene) determined by charge-transfer electronic photodissociation spectroscopy.

Previous Ag$^+$(benzene) CID results from the Armentrout group determined a dissociation limit of 37.4 ± 1.7 kcal/mol and the Duncan group used VMI to obtain a 28.9 ± 3.2 kcal/mol. The VMI result was expected to be lower than the CID result due to the subtraction of the kinetic energy release (KER). The dissociation limit in this experiment was determined to be 75.4 kcal/mol. This higher energy is the result of Frank-Condon factors and excitation to the repulsive wall of the charge-transfer excited states. Ag$^+$(toluene) followed a similar trend with previous VMI results of 35.9 ± 3.2 kcal/mol and a charge-transfer photodissociation threshold of 73.8 kcal/mol. **Figure 12** compares the limit of dissociation for both charge-transfer cation-π complexes.

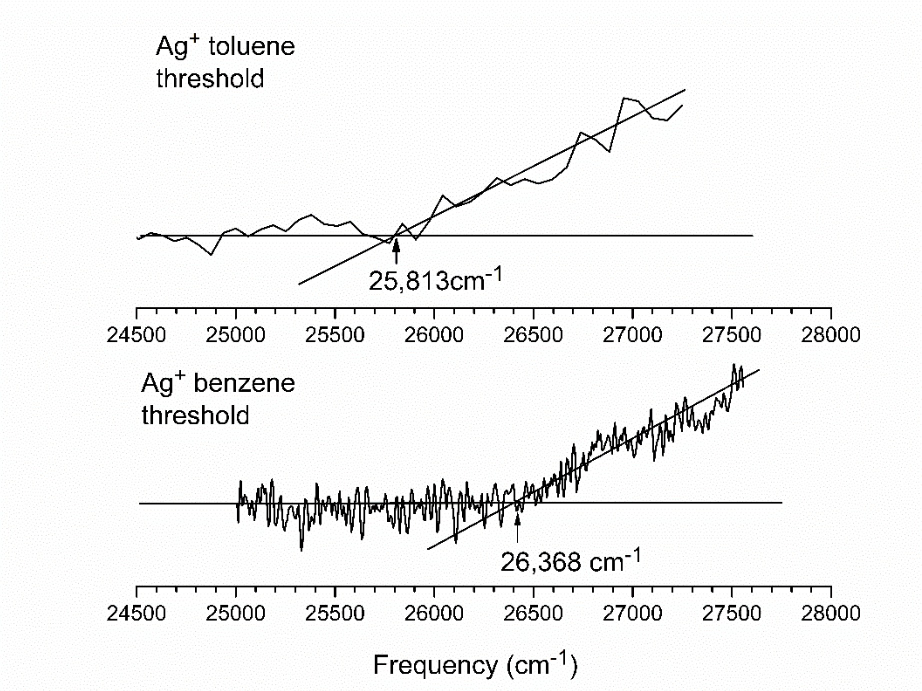

Figure 12: Limit of dissociation for Ag^+(toluene) and Ag^+(benzene) complexes.

CHAPTER 4

COMPUTATIONAL WORK

Methodology

Density functional theory (DFT) has been used historically to predict vibrational and electronic transitions for an expansive range of molecules. Implementing a time-dependent parameter for a classic DFT computations allowed for predictions of excited state electronic transitions. Computations of the structures and bond energies of Ag^+(benzene) and Ag^+(toluene) were completed using DFT with B3LYP and M06-L functionals and def2-TZVP and def2-QZVP basis sets. The excited state theory was completed using TD-DFT with CCSD and def2-TZVP basis set with an added time-dependent parameter. These computations employed the Gaussian 16 program package.[62]

Ag^+(benzene)

Computations of the structures and bond energies of Ag^+(benzene) were completed using computational methods described in the previous section. Ag^+(benzene) was determined to have only one stable structure with the silver ion centered over a carbon-carbon bond on the benzene ring as seen in **Figure 13** below.

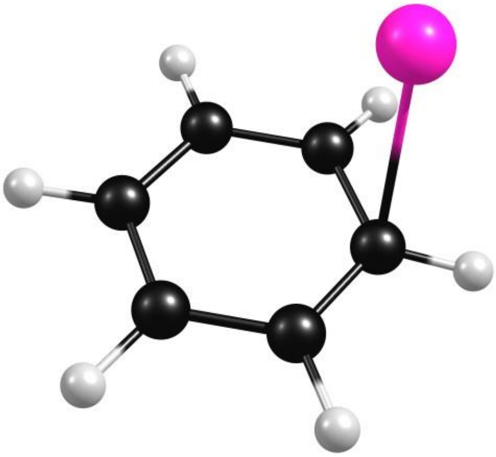

Figure 13: Structure of Ag^+(benzene) generated by TD-DFT computations.

Bond energies are noted in **Table 1** along with previously documented values from literature. The TD-DFT results were used to compare the experimental electronic structure with predicted excited states in order to better understand the electronic structure. **Figure 14** below compares the experimental electronic spectrum of Ag^+(benzene) with the predicted excited states for TD-DFT.

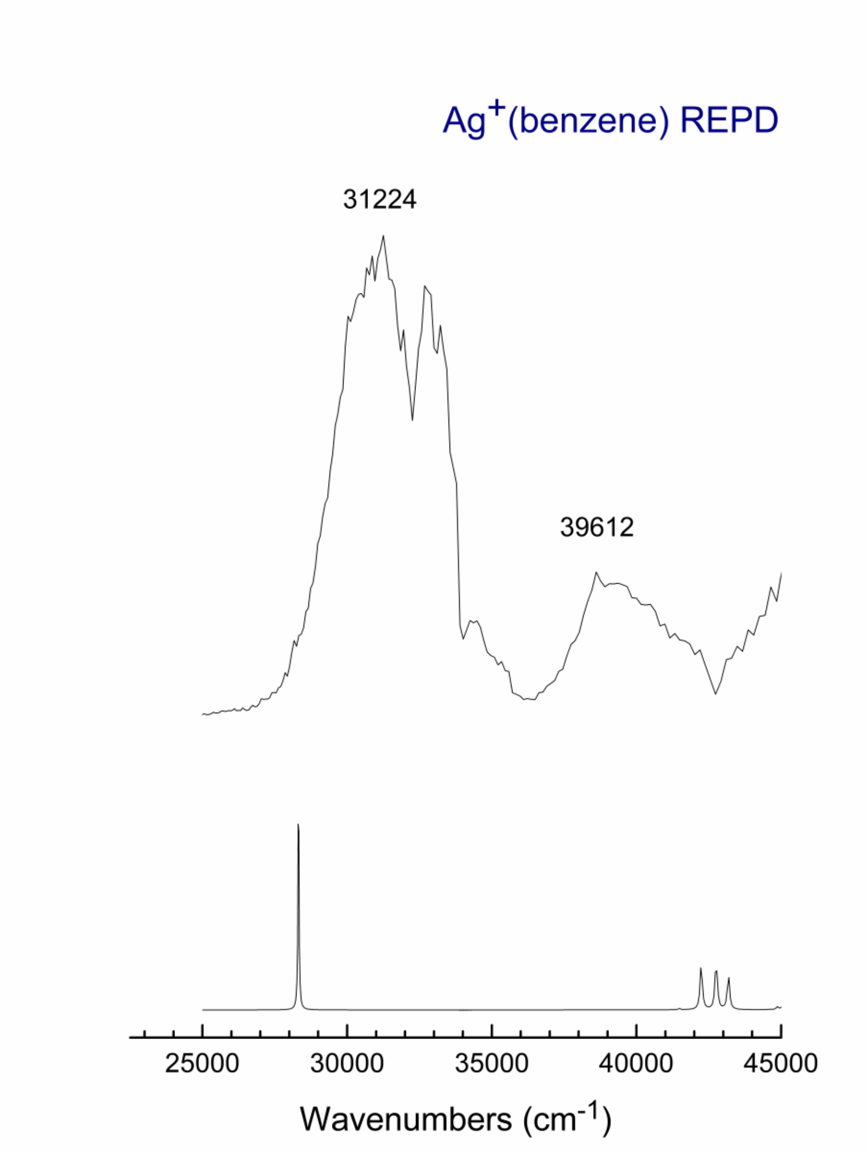

Figure 14: Ag$^+$(benzene) experimental electronic spectrum (top) compared to TD-DFT computational electronic spectrum (bottom).

Four peaks were predicted in the 25,000-45,000 cm^{-1} range using TD-DFT; one peak at 28,255 cm^{-1} and three peaks close in proximity at 42,207 cm^{-1}, 42,752 cm^{-1}, and 43,182 cm^{-1}.

The lower energy absorption at 28,255 cm^{-1} was a straightforward assignment. It was assigned as the charge-transfer transition. It was expected to be an intense, broad absorption and the predicted transition was in the range of the experimental absorption. The higher energy absorption was a little more difficult to assign until looking at the excited state theory. Originally it was proposed that this was a transition from a neutral benzene ligand since no Ag^+ fragment was observed during photodissociation. Looking further into the TD-DFT predicted electronic transition gave insight into what these peaks were. The higher energy peaks lined up relatively close to the experimental 39,612 cm^{-1} peak and predicted an Ag^+ excited state. Looking at the literature values from NIST of the silver excited states in combination with the computations, it was determined the 39,612 cm^{-1} absorption correlated to the Ag^+ $4d^9(^2D_{5/2})5s$ excited state which has a documented frequency of 39,168.0177 cm^{-1}. This is quite odd because only the benzene ion was recorded in photodissociation so there is some unique chemistry occurring from electronic curve crossing.

Ag^+(toluene)

Computations of the structures and bond energies of Ag^+(toluene) were completed using the same computational methods for Ag^+(benzene) as described in the previous section. Ag^+(toluene) was determined to have two stable isomers with the silver ion centered over the 4,5 and 5,6 carbon-carbon bonds on the ring as seen in **Figure 15** below.

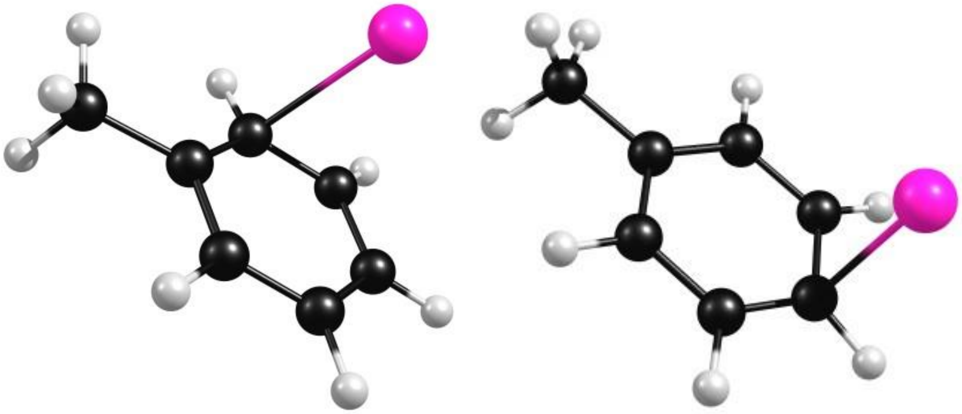

Figure 15: Structure of Ag$^+$(toluene) isomers generated by TD-DFT computations.

Bond energies for both isomers are noted in **Table 2** along with a comparison to literature values. The TD-DFT results were used to compare the experimental electronic structure with predicted excited states in order to better understand the electronic structure. **Figure 16** below compares the experimental electronic spectrum of Ag$^+$(toluene) with the predicted transitions for TD-DFT.

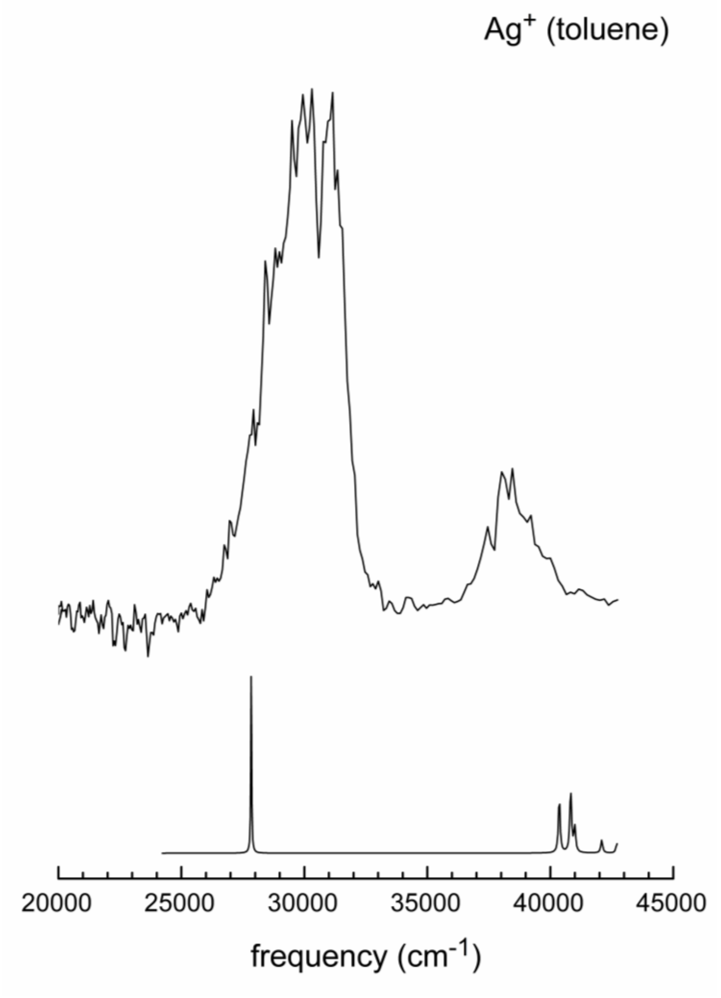

Figure 16: Ag$^+$(toluene) experimental electronic spectrum (top) compared to TD-DFT computational electronic spectrum (bottom).

Three peaks were predicted in the 20,000-42,500 cm^{-1} range using TD-DFT; one absorption at 27,854 cm^{-1} and three absorptions close in proximity at 40,335 cm^{-1}, 40,844 cm^{-1}, and 42,075 cm^{-1}.

The lower energy absorption at 27,854 cm^{-1} was a straightforward assignment. It was assigned as the charge-transfer transition. It was expected to be an intense, broad absorption and the predicted absorption was in the range of the experimental absorption. The higher energy absorptions were a little easier to assign due to them being in close proximity to the documented experimental absorption and also knowing Ag$^+$(benzene) had similar absorptions that were already assigned. Since it was known the absorption for Ag$^+$(benzene) was not a neutral benzene transition, a similar approach was used for assignment. Looking further into the TD-DFT predicted electronic transition gave insight into what these peaks were. The higher energy peaks lined up relatively close to the experimental 38,417 cm^{-1} absorption close to the experimental 39,612 cm^{-1} Ag$^+$(benzene) absorption. Since the common component in both of these complexes is Ag$^+$, this further proved that both higher energy experimental peaks for both complexes must be from the 39,168.0177 cm^{-1} Ag$^+$ 4d^9(^{2}D$_{5/2}$)5s excited state. Looking further to the future it is possible to use this version of TD-DFT to predict charge-transfer excited states as well as metal ion excited electronic transitions. Further research is needed to more accurately determine the chemical dynamics of obtaining an Ag$^+$ electronic excited state from measuring a benzene ion fragment.

Table 2: Computational results for dissociation limits compared to experimental results and previous experiments from literature.

	B3LYP		**M06L**		**Comparison**			
	def2-TZVP	def2-QZVP	def2-TZVP	def2-QZVP	VMI	CID	UV lamp	Experiment
Ag+(benzene)	37.83	38.30	36.58	37.53	< 28.9 ± 3.2	37.4 ± $^{1.7}$	55 ± 5	75.4
Ag+(toluene) Isomer 1	40.86	41.38	39.38	40.29	< 35.9 ± 3.2	n/a	58 ± 5	73.8
Ag+(toluene) Isomer 2	40.03	40.55	38.92	39.84				

REFERENCES

1. J. W. Caldwell, P. A. Kollman, "Cation-π Interactions: Nonadditive Effects Are Critical in their Accurate Representation," *J. Am. Chem. Soc.* **117**, 4177–4178 (1995).
2. D. A. Dougherty, "Cation-π Interactions in Chemistry and Biology. A New View of Benzene, Phe, Tyr, and Trp," *Science* **271**, 163–168 (1996).
3. N. S. Scrutton, A. R. C. Raine, "Cation-π Bonding and Amino-Aromatic Interactions in the Biomolecular Recognition of Substituted Ammonium Ligands," *Biochem. J.* **319**, 1–8 (1996).
4. J. C. Ma, D. A. Dougherty, "The Cation-π Interaction," *Chem. Rev.* **97**, 1303–1324 (1997).
5. J. P. Gallivan, D. A. Dougherty, "Cation-π Interactions in Structural Biology," *Proc. Natl. Acad. Sci. U. S. A.* **96**, 9459–9464 (1999).
6. J. P. Gallivan, D. A. Dougherty, "A Computational Study of Cation-π Interactions vs. Salt Bridges in Aqueous Media: Implications for Protein Engineering," *J. Am. Chem. Soc.* **122**, 870–874 (2000).
7. A. S. Mahadevi, G. N. Sastry, "Cation-π Interaction: Its Role and Relevance in Chemistry, Biology, and Materials Science," *Chem. Rev.* **113**, 2100–2138 (2013). DOI: 10.1021/cr300222d.
8. D. A. Dougherty, "The Cation-π Interaction," *Acc. Chem. Res.* **46**, 885–893 (2013). DOI: 10.1021/ar300265y.

9. C. R. Kennedy, S. Lin, E. N. Jacobsen, "The Cation-π Interaction in Small-Molecule Catalysis," *Angew. Chem. Int. Ed.* **55**, 12596–12624 (2016). DOI: 10.1002/anie.201600547.

10. A. J. Neel, M. J. Hilton, M. S. Sigman, F. D. Toste, "Exploiting Non-Covalent Cation-π Interactions for Catalyst Design," *Nature* **543**, 637–646 (2017). DOI: 10.1038/nature21701.

11. Rutledge, L. R.; Campbell-Verduyn, L. S.; Wetmore, S. D. Characterization of the Stacking Interactions Between DNA Or RNA Nucleobases and the Aromatic Amino Acids. *Chem. Phys. Lett*. **2007**, *444*, 167–175.

12. Burley, S. K.; Petsko, A. G. Aromatic-Aromatic Interaction: A Mechanism of Protein Structure Stabilization. *Science* **1985**, *229*, 23–28.

13. J. Molina, J.A. Dobado, S. Melchor, "Structural and electronic effects of the interaction of metal cations with benzene," Theochem. 589 (2002) 337.

14. M. Diefenbach, C. Trage and H. Schwarz, "Interactions of atomic iron cation with pyridine and benzene: A theoretical study on an unresolved controversy of bond energies and electronic ground-state structures," *Helv. Chim. Acta* 86 (2003) 1008.

15. D. Kim, S. Hu, P. Tarakeshwar, K.S. Kim, J.M. Lisy, "Cation-π interactions: a theoretical investigation of the interaction of metallic and organic cations with alkenes, arenes, and heteroarenes," J. Phys. Chem. A. 107 (2003) 1228.

16. Y. Mokrousov, N. Atodiresei, G. Bihlmayer, S. Bluegel, "Magnetic anisotropy energies of metal - benzene sandwiches," Int. J. Quant. Chem. 106 (2006) 106.

17. T.D. Jaeger, M.A. Duncan, "Photodissociation of M^+(benzene)$_x$ complexes (M=Ti, V, Ni) at 355 nm," Int. J. Mass. Spectrom. 241 (2005) 165.

18. T.D. Jaeger, M.A. Duncan, "Vibrational Spectroscopy of Ni^+(benzene)$_n$ Complexes in the Gas Phase," J. Phys. Chem. A 109 (2005) 3311.

19. Kurikawa, T.; Takeda, H.; Hirano, M.; Judai, K.; Arita, T.; Nagao, S.; Nakajima, A.; Kaya, K. Electronic Properties of Organometallic Metal-Benzene Complexes [M_n(benzene)$_m$ (M = Sc–Cu)]. *Organometallics* **1999**, *18*, 1430–1438.

20. Jaeger, T. D.; Van Heijnsbergen, D.; Klippenstein, S. J.; von Helden, G.; Meijer, G.; Duncan, M. A. Vibrational Spectroscopy and Density Functional Theory of Transition-Metal Ion-Benzene and Dibenzene Complexes in the Gas Phase. *J. Am. Chem. Soc*. **2004**, *126*, 10981–10991 .

21. Zheng, W.; Eustis, N. S.; Li, X.; Nilles, J. M.; Thomas, O. C.; Bowen, K. H.; Kandalam, A. K. Photoelectron Spectroscopic Study of Iron-Benzene Cluster Anions. *Chem. Phys. Lett*. **2008**, *462*, 35–39.

22. Duncan, M. A. Structure, Energetics and Spectroscopy of Gas Phase Transition Metal Ion-Benzene Complexes. *Int. J. Mass Spectrom*. **2008**, *272*, 99 – 118 .

23. Schröder, D.; Brown, R.; Schwerdtfeger, P.; Schwarz, H. Kinetics of radiative/termolecular associations in the low pressure regime: reactions of bare Au1 with benzene. *Int. J. Mass Spectrom.* **2000**, *203*, 155–163

24. Butschke, B.; Schwarz, H. Thermal C-H Bond Activation of Benzene, Toluene, and Methane with Cationic [M(X)(bipy)]þ (M=Ni, Pd, Pt;X=CH_3, Cl; bipy = 2,20-bipyridine): A Mechanistic Study. *Organometallics* **2011**, *30*, 1588–1598.

25. Caraiman, D.; Bohme, D. K. Periodic Trends in Reactions of Benzene Clusters of Transition Metal Cations, $M(C_6H_6)_{1,2}^+$, with Molecular Oxygen. *J. Phys. Chem. A* **2002**, *106*, 9705-9717.

26. Caraiman, D.; Bohme, D. K. The gas-phase chemistry of iron cations coordinated to benzene and the extended aromatic coronene. *Int. J. Mass Spectrom*. **2003**, 223–224, 411–425.

27. Amicangelo, J. C.; Armentrout, P. B. Absolute Binding Energies of Alkali-Metal Cation Complexes with Benzene Determined by Threshold Collision-Induced Dissociation Experiments and ab Initio Theory. *J. Phys. Chem. A* **2000**, *104*, 11420-11432.

28. Jaeger, T. D., Duncan, M. A. Vibrational Spectroscopy of $Ni^+(benzene)_n$ Complexes in the Gas Phase. *J. Phys. Chem. A* **2005**, *109*, 3311–3317.

29. Pandey, R.; Rao, B. K.; Jena, P.; Newsam, J. M. Unique Magnetic Signature of Transition Metal Atoms Supported on Benzene. *Chem. Phys. Lett*. **2000**, *321*, 142–150.

30. Grover, J. R.; Walters, E. A.; Hui, E. T. Dissociation Energies of the Benzene Dimer and Dimer Cation. *J. Phys. Chem*. **1987**, *91*, 3233–3237.

31. Krause, H.; Ernstberger, B.; Neusser, H. J. Binding Energies of Small Benzene Clusters.

32. *Chem. Phys. Lett*. **1991**, *184*, 411–417.

33. Jorgensen, W. L.; Severance, D. L. Aromatic-Aromatic Interactions: Free Energy Profiles for the Benzene Dimer in Water, Chloroform, and Liquid Benzene. *J. Am. Chem. Soc.* **1990**, *112*, 4768–4774.

34. Hobza, P.; Selzle, H. L.; Schlag E. W. Potential Energy Surface for the Benzene Dimer. Results of *ab Initio* CCSD(T) Calculations Show Two Nearly Isoenergetic Structures: T-Shaped and Parallel-Displaced. *J. Phys. Chem*. **1996**, *100*, 18790–18794.

35. Henson, B. F.; Hartland, G. V.; Venturo, V. A.; Felker, P. M. Raman–Vibronic Double-Resonance Spectroscopy of Benzene Dimer Isotopomers. *J. Chem. Phys*. **1992**, *97*, 2189–2208.

36. Arunan, E.; Gutowsky, H. S. The Rotational Spectrum, Structure and Dynamics of a Benzene Dimer. *J. Chem. Phys*. **1993**, *98*, 4294–4296.

37. Ebata, T.; Hamakado M.; Moriyama, S.; Morioka, Y.; Ito, M. Raman Depolarization Ratios of Jet-Cooled Benzene and its Dimer by Stimulated Raman–UV Optical Double-Resonance Spectroscopy. *Chem. Phys. Lett*. **1992**, *199*, 33–41.

38. Janowski, T.; Pulay, P. High Accuracy Benchmark Calculations of the Benzene Dimer Potential Energy Surface. *Chem. Phys. Lett*. **2007**, *447*, 27–32.

39. Kusaka, R.; Inokuchi, Y.; Ebata, T. Vibrational Energy Relaxation of Benzene Dimer and Trimer in the CH Stretching Region Studied by Picosecond Time-Resolved IR-UV Pump-Probe Spectroscopy. *J. Chem. Phys*. **2012**, *136*, 044304/1–11.

40. Van der Avoird, A.; Podeszwa, R.; Szalewicz, K.; Leforestier, C.; Van Harrevelt, R.; Bunker, P. R.; Schnell, M.; Von Helden, G.; Meijer, G. Vibration-Rotation-Tunneling States of the Benzene Dimer: An *Ab Initio* Study. *Phys. Chem. Chem. Phys*. **2010**, *12*, 8219–8240.

41. Meyer, F.; Khan, F. A.; Armentrout, P. B. Thermochemistry of Transition Metal Benzene Complexes: Binding Energies of $M(C_6H_6)_x^+$ (x = 1,2) for M = Ti to Cu. *J. Am. Chem. Soc*. **1995**, *117*, 9740–9748.

42. Bauschlicher, C. W., Jr.; Partridge, H.; Langhoff, S. R. Theoretical Study of Transition-Metal Ions Bound to Benzene. *J. Phys. Chem*. **1992**, *96*, 3273–3278.

43. Pandey, R.; Rao, B. K.; Jena, P.; Alvarez-Blanco, M. Electronic Structure and Properties of Transition Metal-Benzene Complexes. *J. Am. Chem. Soc*. **2001**, *123*, 3799–3808.

44. Wedderburn, K. M.; Bililign, S.; Levy, M.; Gdanitz, R. J. Geometries and Stabilities of 3d-Transition Metal-Cation Benzene Complexes, M^+Bz_n (M = Sc–Cu, n = 1,2). *Chem. Phys.* **2006**, *326*, 600–604.

45. Daunt, S. J.; Shurvell, H. F. Infrared Band Contours of Benzene and Benzene-d6. *Spectrochim. Acta* **1975**, *32A*, 1545–1552.

46. Snavely, D. L.; Walters, V. A.; Colson, S. D.; Wiberg, K. B. FTIR Spectrum of Benzene in a Supersonic Expansion. *Chem. Phys. Lett*. **1984**, *103*, 423–429

47. C. Yang, S. J. Klippenstein, "Theory and Modeling of the Binding in Cationic Transition-Metal - Benzene Complexes," J. Phys. Chem. A 103 (1999) 1094. b) S. J. Klippenstein, C. Yang, "Density functional theory predictions for the binding of transition metal cations to pi systems: From acetylene to coronene to tribenzocyclyne," Int. J. Mass Spec. 201 (2000) 253.

48. T.K. Dargel, R.H. Hertwig, W. Koch, "How do coinage metal ions bind to benzene?" Mol. Phys. 96 (1999) 583.

49. R. Pandey, B.K. Rao, P. Jena, J.M. Newsam, "Unique magnetic signature of transition metal atoms supported on benzene," Chem. Phys. Lett. 321 (2000) 142.

50. G. Hong, M. Dolg, L. Li, "Scalar-relativistic density functional and ab initio pseudopotential study of zero-valent d and f metal bis-□ 6- benzene sandwich complexes M(C6H6)2 (M = Sc, Ti, Y, Zr, La, Lu, Hf, Th, U)," Int. J. Quant. Chem. 80 (2000) 201.

51. M. Dolg, "Combined Pseudopotential and Density Functional Study of Bis-eta^6-benzene d and f Element complexes," J. Chem. Inf. Comput. Sci. 41 (2001) 18.

52. R. Pandey, B.K. Rao, P. Jena, M.A. Blanco, "Electronic structure and properties of transition metal - benzene complexes," J. Am. Chem. Soc. 123 (2001) 3799.

53. P. Chaquin, D. Costa, C. Lepetit, M. Che, "Structure and Bonding in a Series of Neutral and Cationic Transition Metal-Benzene η6 Complexes [M(η 6-C6H6)]*n*+ (M) Ti, V, Cr, Fe, Co, Ni, and Cu). Correlation of Charge Transfer with the Bathochromic Shift of the E1 Ring Vibration," J. Phys. Chem. A 105 (2001) 4541.

54. H. Higashide, T. Kaya, M. Kobayashi, H. Shinohara, H. Sato, "Reactions of benzene clusters with metal ions as studied by the laser ablation-molecular beam method: Observation of clusters complex ions $M(C_6H_6)_n^+$ ($n \geq 2$) and fragment complex ions $M(C_6H_6)(C_xH_y)^+$ with $x \leq 6$ and $y \leq 4$," Chem. Phys. Lett. 171 (1990) 297.

55. C. Berg, M. Beyer, U. Achatz, S. Joos, G. Niedner-Schatteburg, V. E. Bondybey, "Effect of charge upon metal cluster chemistry: Reactions of Nbn and Rhn anions and cations with benzene," J. Chem. Phys. 108 (1998) 5398.

56. K. Hoshino, T. Kurikawa, H. Takeda, A. Nakajima, K. Kaya, "Structures and Ionization Energies of Sandwich Clusters (Vn(benzene)m)," J. Phys. Chem. 99 (1995) 3053.

57. K. Hoshino, T. Kurikawa, H. Takeda, A. Nakajima, K. Kaya, "Structures of organometallic clusters: V_n(benzene $)_m$ and Co_n(benzene $)_m$," Surf. Rev. Lett. 3 (1996) 183.

58. W. Zheng, J.M. Nilles, O.C. Thomas, K.H. Bowen, Jr., "Photoelectron spectroscopy of nickel- benzene cluster anions," J. Chem. Phys. 122 (2005) 044306.

59. W. Zheng, J.M. Nilles, O.C. Thomas, K.H. Bowen, Jr., "Photoelectron spectroscopy of titanium- benzene cluster anions," Chem. Phys. Lett. 401 (2005) 266.

60. B.R Sohnlein, S. Li, D.-S. Yang, "Electron-spin multiplicities and molecular structures of neutral and ionic scandium- benzene complexes," J. Chem. Phys. 123 (2005) 214306.

61. B.R. Sohnlein, D.-S. Yang, "Pulsed-field ionization electron spectroscopy of group 6 metal (Cr, Mo, and W) bis(benzene) sandwich complexes," J. Chem. Phys. 124 (2006) 134305.

62. Frisch, M. J.; Trucks, G. W.; Schlegel, H. B.; Scuseria, G. E.; Robb, M. A.; Cheeseman, J. R.; Scalmani, G.; Barone, V.; Peterson, G. A.; Nakatsuji, H. et al. *Gaussian16,* Gaussian, Inc.; Wallingford, CT, **2009**.

63. Chen, Y.-M.; Armentrout, P. B. Collision-Induced Dissociation of $Ag(C_6H_6)^+$. *Chem. Phys. Lett*. **1993**, *210*, 123−128.

64. J. E. Reddic and M. A. Duncan, "Photodissociation spectroscopy of Mg+-C2H2," Chem. Phys. Lett. 312, 96-100 (1999).

65. M. R. France, S. H. Pullins and M. A. Duncan, "Photodissociation spectroscopy of Ca+-C2H2 and Ca+-C2D2 p-complexes," J. Chem. Phys. 109, 8842-8850 (1998).

66. Yang, Y.-S.; Yeh, C.-S. Photodissociative Charge Transfer in Ag^+-Pyridine Complex. *Chem. Phys. Lett.* **1999**, *305*, 395–400.

67. Yang, Y.-S.; Hsu, W.-Y.; Lee, H.-F.; Huang, Y.-C.; Yeh, C.-S. Experimental and Theoretical Studies of Metal Cation-Pyridine Complexes Containing Cu and Ag. *J. Phys. Chem. A* **1999**, *103*, 11287–11292.

68. Su, P. H.; Yeh, C. S. Photofragmentation of the Ag^+-Furan Complex in the Gas-Phase. *Chem. Phys. Lett.* **2000**, *331*, 420–424.

69. Su, P. H.; Lin, F. W.; Yeh, C. S. Photodissociation Studies of $M(Furan)^+$ (M = Cu, Ag, and Au) and $Au(C_3H_4)^+$ Complexes. *J. Phys. Chem. A* **2001**, *105*, 9643–9648.

70. Chen, J.; Wong, T. H.; Cheng, Y. C.; Montgomery, K.; Kleiber, P. D. Photodissociation Spectroscopy and Dynamics of $MgC_2H_4^+$. *J. Chem. Phys.* **1998**, *108*, 2285–2296.

71. Lu, W.-Y; Kleiber, P. D.; Young, M. A. Photodissociation Spectroscopy of $Zn^+(C_2H_4)$. *J. Chem. Phys.* **2001**, *115*, 5823–5829.

72. Maner, J. A.; Mauney, D. T.; Duncan, M. A. Imaging Charge Transfer in a Cation-π System: Velocity-Map Imaging of Ag^+(benzene) Photodissociation. *J. Phys. Chem. Lett.* **2015**, *6*, 4493–4498.

73. Jarrold, M. F.; Misev, L.; Bowers, M. T. Charge Transfer Half-Collisions: Photodissociation of the $Kr{\cdot}O_2^+$ Cluster Ion with Resolution of the O_2 Product Vibrational States. *J. Chem. Phys.* **1984**, *81*, 4369–4379.

74. Illies, J. I.; Jarrold, M. F.; Wagner-Redeker, W.; Bowers, M. T. Photoinduced Intramolecular Charge Transfer: Photodissociation of $CO_2^+{\cdot}Ar$ Cluster Ions. *J. Am. Chem. Soc.* **1985**, *107*, 2842–2849.

75. Kim, H.-S.; Kuo, C.-H.; Bowers, M. T. Photon Driven Charge Transfer Half Collisions: The Photodissociation of $CO_2^+{\cdot}O_2$ Cluster Ions with Resolution of the O_2 Product Vibrational States. *J. Chem. Phys.* **1987**, *87*, 2667–2676.

76. Willey, K. F.; Cheng, P. Y.; Pearce, K. D.; Duncan, M. A. Photoinitiated Charge Transfer and Dissociation in Mass-Selected Metallo-Organic Complexes. *J. Phys. Chem***.** **1990**, *94,* 4769−4772.

77. Willey, K. F.; Cheng, P. Y.; Bishop, M. B.; Duncan, M. A. Charge-Transfer Photochemistry in Ion-Molecule Cluster Complexes of Silver. *J. Am. Chem. Soc.* **1991**, *113*, 4721−4728.

78. Willey, K. F.; Yeh, C. S.; Robbins, D. L.; Duncan, M. A. Charge Transfer in the Photodissociation of Metal Ion-Benzene Complexes. *J. Phys. Chem.* **1992**, *96*, 9106−9111.

79. Jaeger, T. D.; Duncan, M. A. Photodissociation of M^+(benzene)$_x$ Complexes (M = Ti, V, Ni) at 355 nm. *Int. J. Mass Spectrom.* **2005**, *241*, 165−171.

80. B. M. Rittgers, D. Leicht, M. A. Duncan. Cation-π Complexes of Silver Studied with Photodissociation and Velocity-Map Imaging," J. Phys. Chem. A 124, 9166-9176 (2020).

81. A. Kramida. A Critical Compilation of Energy Levels, Spectral Lines, and Transition Probabilities of Singly Ionized Silver, Ag II. *J. Res. Natl. Inst. Stand. Technol*. **2013**, *1128*, 168-198.

82. Afzaal, S.; Freiser, B. S. Gas-phase Photodissociation Study of Ag(benzene)$^+$ and Ag(toluene)$^+$. *Chem. Phys. Lett.* **1994**, *218*, 254–260.

83. D. Schroeder, J. Hrus´ak, R.H. Hertwig, W. Koch, P. Schwerdtfeger, H. Schwarz, Organometallics 14 **1995,** 312.